

# RSC Advances



This is an *Accepted Manuscript*, which has been through the Royal Society of Chemistry peer review process and has been accepted for publication.

*Accepted Manuscripts* are published online shortly after acceptance, before technical editing, formatting and proof reading. Using this free service, authors can make their results available to the community, in citable form, before we publish the edited article. This *Accepted Manuscript* will be replaced by the edited, formatted and paginated article as soon as this is available.

You can find more information about *Accepted Manuscripts* in the [Information for Authors](#).

Please note that technical editing may introduce minor changes to the text and/or graphics, which may alter content. The journal's standard [Terms & Conditions](#) and the [Ethical guidelines](#) still apply. In no event shall the Royal Society of Chemistry be held responsible for any errors or omissions in this *Accepted Manuscript* or any consequences arising from the use of any information it contains.

1 **Mechanism of cement paste reinforced by graphene oxide/ carbon nanotubes composites**  
2 **with enhanced mechanical properties**

3 Zeyu LU<sup>1</sup>, Lingshi MENG<sup>1</sup>, Guoxing SUN<sup>1</sup>, Cong LU<sup>1</sup>, Dongshuai HOU<sup>2\*</sup>, Zongjin LI<sup>1</sup>

4

5 1.Department of Civil and Environmental Engineering, The Hong Kong University of Science  
6 and Technology, Hong Kong, China.

7 2.Department of Civil Engineering, Qingdao Technological University (Cooperative Innovation  
8 Center of Engineering Construction and Safety in Shandong Blue Economic Zone), Qingdao,  
9 China

10 Tel.: +852-9162-6614; Fax: +852-2358-1534.

11

12 \* Corresponding author: Dongshuai HOU; E-mail: monkeyphildhou@gmail.com

13

14

### **Abstract**

15 This paper presents the enhanced mechanical properties of cement paste reinforced by graphene  
16 oxide (GO)/ carbon nanotubes (CNTs) composites. The UV-vis spectroscopy and optical  
17 microscopy results showed that the dispersion of CNTs in the GO solution is much better than in  
18 an aqueous solution due to the higher electrostatic repulsion, which allows a completely new  
19 approach of dispersing CNTs rather than by incorporating a dispersant. More importantly, the  
20 GO/CNTs composite plays an important role in improving the compressive and flexural strength  
21 of cement paste by 21.13 % and 24.21 %, which is much higher than cement paste reinforced by  
22 CNTs (6.40 % and 10.14 %) or GO (11.05 % and 16.20 %), respectively. The improved  
23 mechanical properties of cement paste is attributed to the better dispersed CNTs and enhanced

24 interactions among CNTs by the GO incorporation. Finally, the space interlocking mechanism of  
25 the GO/CNTs/cement paste composite with enhanced mechanical properties was proposed.

26 Keywords: Graphene oxide; Carbon nanotubes; Mechanical properties; Cement paste.

27

## 28 **1. Introduction**

29 Brittleness and lack of flexural/tensile strength are the two major limitations of cementitious  
30 materials [1]. Traditional methods to improve the flexural/ tensile strength of cementitious  
31 materials include introducing fibers, such as steel fibers, carbon fibers and polyvinyl alcohol  
32 (PVA) fibers, which can significantly enhance the crack-resistance of cement and restrain crack  
33 propagation in the macro scale. Another effective way is to combine cementitious materials with  
34 nanomaterials, such as nano-silica, carbon nanotubes (CNTs) and graphene oxide (GO). Since  
35 CNTs and GO possess a high elastic modulus and tensile strength, the use of these carbon  
36 nanomaterials to strengthen cementitious composites has attracted most concerns recently.

37

38 CNTs, including single wall (SWCNTs) or multi walls (MWCNTs), are one-dimensional carbon  
39 nanomaterial that may be viewed as rolled up from a single planar sheet of graphene. The unique  
40 mechanical properties make it as an attractive candidate for reinforcement of composite  
41 materials. Many attempts have been made to incorporate CNTs as reinforcement in cementitious  
42 materials and to investigate the mechanical behavior. However, the prerequisite for CNTs  
43 reinforcement is the uniform dispersion of CNTs. Three major methods for dispersing CNTs are  
44 the addition of surfactants, mechanical ultrasonication and functionalization of CNTs. Shah et al.  
45 [2] investigated the effects of ultrasonic energy and surfactant concentration on the dispersion of

46 MWCNTs at an amount of 0.08 wt. % of cement, and found that the appropriate dispersion of  
47 CNTs could be achieved by using sonication and a surfactant-to-CNTs weight ratio of 4. Konsta-  
48 Gdoutous et al. [3] demonstrated that the flexural strength of the cement paste with the addition  
49 of MWCNTs at a concentration of 0.08 % was improved by 35 % with the help of surfactants  
50 and ultrasonication. Shama et al. [4] indicated that 0.1 wt. % of SWCNTs improved flexural  
51 modulus, flexural strength and compressive strengths of mortar by 72%, 7 % and 19 %, through  
52 a short dispersion route using Pluronic F-127 as a novel dispersing agent. Duan et al. [5]  
53 demonstrated that the flexural strength, Young's modulus and fracture toughness of cement paste  
54 were significantly improved by using 0.55 wt. % CNTs with a pre-treatment of 50 J/mL  
55 ultrasonication energy. Although the addition of surfactants contributes to better dispersion of  
56 CNTs in cementitious materials, it has a weak interface between CNTs and cement matrix.  
57 Moreover, ultrasonication dispersion of CNTs before mixing with the cement matrix makes it  
58 more expensive, complicated and time-consuming, and excessive ultrasonication has damage  
59 effects on the properties of CNTs. Furthermore, defect free CNTs are incapable of forming good  
60 adhesion with the cement matrix. Even if better dispersion of the CNTs can be obtained with the  
61 help of surfactants, the sliding of the CNTs still readily occurs due to the weak bonding between  
62 the CNTs and matrix, which leads to the poor reinforcing effect on the mechanical behavior of  
63 cementitious materials. Therefore, chemical functionalization of CNTs has been widely  
64 investigated and developed because of the improved chemical bonding between CNTs and the  
65 cementitious matrix. Cwirzen et al. [6] investigated the surface decoration of MWCNTs on the  
66 mechanical properties of cement paste and indicated that the compressive strength can be  
67 improved to nearly 50 % with only a small addition (0.045-0.15 wt. %) of MWCNTs. Li et al.  
68 [7] showed that the use of chemically functionalized CNTs in a concentration of 0.5 % by weight

69 of cement led to an increase in the compressive and flexural strength of cement mortar of 19 %  
70 and 25 %, respectively. However, the reinforcing efficiency of chemical functionalization of  
71 CNTs on the mechanical properties of cementitious materials greatly depends on the following  
72 two points: 1) dispersion of the functionalized CNTs. Although functionalized CNTs shows  
73 better dispersion in an aqueous solution than pure CNTs, because of the hydrophilic functional  
74 groups, it still needs to be improved because better dispersion of CNTs leads to better mechanical  
75 properties of the cementitious materials. The increasing concentration of functionalized CNTs  
76 may lead to further mechanical improvement of cementitious materials, but the agglomeration  
77 more readily occurs with excessive CNTs content, so how to improve the dispersion of  
78 functionalized CNTs with a fixed concentration is important. 2) damage of the functionalized  
79 CNTs. The mechanical properties of the functionalized CNTs are not as good as pure CNTs due  
80 to structure damage. There is a trade-off between the improved chemical interactions of  
81 functionalized CNTs/cement matrix and the decreased mechanical properties of the  
82 functionalized CNTs itself. Therefore, a question that has arisen is ‘whether there is a way that  
83 not only improves the dispersion of functionalized CNTs but also has a positive effect on the  
84 mechanical properties of cementitious materials which can compensate for the mechanical loss  
85 of the functionalized CNTs’.

86

87 Differing from CNTs, GO is an excellent hydrophilic material with oxygen-containing groups,  
88 such as hydroxyl, carbonyl and carboxyl. Therefore, the dispersion of GO in an aqueous solution  
89 is excellent and therefore, it is much easier to mix with cement compared with CNTs. Duan et al.  
90 [8] demonstrated that the introduction of 0.05 wt. % GO can increase the compressive strength  
91 and flexural strength of GO/cement composite by 33 % and 59 %, respectively. Saafi et al. [9]

92 reported that 0.35 wt. % GO can improve the flexural strength, Young's modulus and flexural  
93 toughness of geopolymeric cement by 134 %, 376 % and 56 %, respectively. The improved  
94 mechanical properties of cementitious composites are mainly attributed to the high specific  
95 surface area and excellent mechanical properties of GO [10].

96

97 Although CNTs and GO make a great contribution to the mechanical enhancement of  
98 cementitious materials, the co-effects of GO/CNTs composites on the mechanical behavior of  
99 cementitious materials have not been investigated. In addition, what might happen if the negative  
100 charged CNTs and GO are combined, and the question as to whether the dispersion of CNTs in a  
101 GO solution can be improved due to the electrostatic repulsion still needs to be settled [11]. In  
102 the present study, the carboxylic functionalization of CNTs were firstly dispersed in a GO  
103 solution and an aqueous solution, respectively, and the dispersion efficiency of the functionalized  
104 CNTs in both solutions were characterized by UV-vis spectroscopy and optical microscopy.  
105 Then, the mechanical behavior and microstructure of cement paste reinforced with 0.05 wt. %  
106 functionalized CNTs, 0.05 wt. % GO and 0.025 wt. % functionalized CNTs/ 0.025 wt. % GO  
107 composite were investigated by mechanical testing and Scanning electron microscopy (SEM)  
108 with energy dispersive X-ray (EDX) spectroscopy technique. The chemical interactions between  
109 functionalized CNTs and GO were investigated by the Fourier transform infrared (FTIR)  
110 technique. Finally, the space interlocking mechanism of the cement paste reinforced with  
111 GO/functionalized CNTs composite with enhanced mechanical property was proposed.

112

## 113 2. Experimental methods

### 114 2.1 Materials

115 Ordinary Portland cement (OPC) type 52.5 (Green island, HK) and Class F were used to  
116 fabricate the cement paste. Carboxylic functionalization of CNTs was used in this study because  
117 it can generate strong chemical bonding between the CNTs and cement matrix [12], which were  
118 provided by the Shenzhen Nanotech Port Co. Ltd in China, and its properties are shown in Table  
119 1. In the following study, the term of CNTs is short for the carboxylic functionalization of CNTs  
120 unless it is expressly stated.

121

122 **Table 1** Properties of CNTs

Diameter (nm)	Length ( $\mu\text{m}$ )	Aspect ratio	Specific surface area ( $\text{m}^2 \cdot \text{g}^{-1}$ )	Electric conductivity ( $\text{s} \cdot \text{cm}^{-1}$ )
40-80	5-15	800	40-300	$(15-30) \times 10^{-3}$

123

### 124 2.2 Preparation of GO

125 GO was prepared from graphite powder (Alfa-Aesar, 200 mesh) according to the modified  
126 Hummer's method (Hummers and Offeman, 1985). Graphite powder (3 g) was added to a  
127 solution containing  $\text{K}_2\text{S}_2\text{O}_8$  (2 g),  $\text{P}_2\text{O}_5$  (2 g) and concentrated  $\text{H}_2\text{SO}_4$  (40 mL, 98 wt. %) for 6 h  
128 mixing at 80 °C. The resulting mixture was then diluted with distilled water, filtered and washed  
129 until the pH value of the rinse water became neutral. The dried graphite oxide was re-dispersed  
130 into concentrated  $\text{H}_2\text{SO}_4$  (100 mL, 98 wt. %) in an ice bath.  $\text{KMnO}_4$  (15 g) was gradually added  
131 and stirred for 2 h. The mixture was then stirred and mixed at 35 °C for another 2 h, followed by  
132 the addition of 230 mL of distilled water. The resultant bright yellow solution was terminated by

133 adding 700 mL of distilled water and 15 mL 30 % H<sub>2</sub>O<sub>2</sub>, and subjected to centrifugation and  
134 careful washing by 37 % HCl and distilled water. After immersing the as-prepared suspension in  
135 dialysis tubing cellulose membranes for 7 days, it was finally centrifuged and collected for  
136 preparing different concentrations of graphene oxide solution. In this study, the concentration of  
137 the GO solution was 1.2 mg/mL. Fig. 1 shows the X-ray diffraction (XRD) pattern of the  
138 graphite and GO used in this study. It clearly indicates that the diffraction peak of graphite and  
139 GO are at 26.72 ° and 10.14 °, respectively. The interlayer spacing ( $d$ ) can be calculated by  
140 Bragg's equation. Compared with graphite ( $d_{\text{graphite}} = 0.34 \text{ \AA}$ ), the  $d_{\text{GO}}$  increases to 0.87 Å due to  
141 the oxygen group addition during the oxidation process, which can enlarge the distance among  
142 different layers of GO. In addition, the oxidation content of the GO was characterized by the X-  
143 ray photoelectron spectroscopy (XPS). Fig. 2 clearly shows four types of carbon bonds in GO,  
144 including the C-C at 284.4 eV, C-O at 286.4 eV, C=O 288.3 at eV and -COOH at 289.0 eV. The  
145 elemental analysis of the XPS results indicate that the C/O ratio and oxygen content of the GO in  
146 this study are 3.0 and 30.7 %, respectively.

147

### 148 **2.3 Preparation and characterization of CNTs suspensions**

149 0.02 g of CNTs was dispersed in 50 mL aqueous solution and GO solution by using a 275 W  
150 ultrasonicator for 15 min, and the two solutions were diluted 100 times before the UV-vis  
151 spectrometer test. The dispersion of CNTs was characterized by using UV-vis spectroscopy  
152 (Lambda 950, Perkin Elmer) with a wavelength range of 190-1100 nm and a typical optical  
153 microscope (BX51, Olympus). The absorbance (ABS) was measured at a specific wavelength of  
154 600 nm.

155

## 156 2.4 Preparation and characterization of the GO/CNTs/cement paste composite

157 0.05 % CNTs by weight of cement paste was dispersed by using 275 W ultrasonicator for 15 min  
158 in the required GO solution before mixing with the cement paste. It should be noted that the  
159 water to cement ratio (w/c) of 0.4 was used for the cement paste, and the water used for  
160 fabrication of GO/CNTs/cement paste composite was totally replaced by the water in the GO  
161 solution, so extra water was not needed. Based on the w/c and concentration of GO solution (1.2  
162 mg/mL), the solid content of GO was 0.05 % by weight of cement paste. The as-prepared  
163 CNTs/GO solution was then mixed with cement in high mixing speed for 10 min, and placed into  
164 steel molds followed by 20 s of vibration. The specimens were then covered under polyethylene  
165 sheets for 24 h in the laboratory environment before demolding. After demolding, the specimens  
166 were cured for 14 days at a temperature of 20 °C and humidity of 98 %.

167

168 For the mechanical property tests, a three-point bending test was conducted following the  
169 procedure prescribed by ASTM C78/C78 M-10. Three specimens with dimensions of 150 mm ×  
170 30 mm × 10 mm were measured with a span of 90 mm and a stroke control at a loading rate of  
171 0.1 mm/min. Two linear variable differential transformers (LVDTs) were set up on each side of  
172 the specimen to measure the mid-point deflection. The compressive strength test was conducted  
173 by testing three cubes of size 40 mm × 40 mm × 40 mm. The samples were placed in a materials  
174 testing system and loaded at the speed of 1 kN/s. FTIR testing was conducted to investigate the  
175 chemical interactions between the CNTs and GO. The microstructures of GO/cement paste  
176 composite and GO/CNTs/cement paste composite were evaluated by the SEM/EDX technique.

177

### 178 3. Results and discussion

#### 179 3.1 Dispersion efficiency of CNTs/aqueous and CNTs/GO solution

180 Fig. 3 shows the UV-vis spectroscopy results of the CNTs/aqueous and CNTs/GO solutions. As  
181 shown in Fig. 3, it is evident that the ABS for the CNTs/GO solution is 3 times higher than that  
182 for CNTs/aqueous solution. On the basis of Beer's law [13], the ABS is proportional to the  
183 dispersed CNTs because only dispersed CNTs can effectively absorb light in the UV-vis region.  
184 Therefore, the dispersion of CNTs in a GO solution is much better than that in an aqueous  
185 solution [14]. The mechanism can be attributed to the larger electrostatic repulsion in the  
186 CNTs/GO solution [11, 15], as shown in Fig. 4. Unfunctionalized CNTs tend to agglomerate due  
187 to the high surface energy, as seen in Fig. 4a. However, functionalized CNTs show better  
188 dispersion in an aqueous solution due to the hydrophilic oxygen-containing groups (-COOH), as  
189 seen in Fig. 4b. The negative charged CNTs repulse each other due to the weak electrostatic  
190 repulsion as a result of ionization of the carboxylic acid groups. More importantly,  
191 functionalized CNTs show the best dispersion in the GO solution due to the electronegativity of  
192 the GO solution itself, which results from the ionization of the phenolic hydroxyl and carboxylic  
193 acid groups. The larger electrostatic repulsion leads to the increased distance among the CNTs,  
194 and thus the best dispersion of functionalized CNTs can be achieved in the CNTs/GO solution, as  
195 seen in Fig. 4c.

196

197 In order to better investigate the dispersion of CNTs in aqueous and GO solutions, a typical  
198 optical microscope test for CNTs/aqueous and CNTs/GO solutions was carried out, and the  
199 results are presented in Fig. 5. Although CNTs are dispersed by a pre-ultrasonication of 15 min,

200 some agglomerates of the CNTs in the aqueous solution are still observed due to the large surface  
201 tension and energy, as seen in Fig. 5a. In contrast, the bundled CNTs disappear and better  
202 dispersion of CNTs can be achieved in the GO solution, as seen in Fig. 5b. The microscope  
203 results are consistent with the UV-vis spectroscopy results, indicating the dispersion of CNTs in  
204 GO solutions is much better than in aqueous solutions.

205

### 206 **3.2 Mechanical properties of the cement paste reinforced by GO and CNTs**

207 The compressive and flexural behavior of cement paste with and without the CNTs and GO  
208 composite is shown in Fig. 6. Table 2 lists the mechanical behavior of cement paste with  
209 different contents of CNTs and GO. It can clearly be seen that the incorporation of 0.05 wt. %  
210 CNTs lead to a 6.40 % increase in compressive strength and 10.14 % in flexural strength of the  
211 cement paste. Moreover, 0.05 % GO shows a similar but stronger reinforcement on cement paste,  
212 leading to a 11.05 % increase in compressive strength and 16.20 % in flexural strength,  
213 indicating that GO can remarkably enhance the mechanical properties of cement paste, which  
214 was also reported in other studies [8, 16-18]. The improved mechanical behavior of the  
215 GO/cement paste composite is attributed to the excellent mechanical properties of the GO itself  
216 and the pore-filling effect of the GO on the cement matrix. In this study, the pore-filling effect of  
217 GO was for the first time investigated by the SEM technique. Fig. 7 shows the SEM/EDX results  
218 of the GO/cement paste. It can clearly be seen that there no GO exists in the highlighted part in  
219 Fig. 7a, and no carbon (C) elements were found based on the EDX results. The pores or voids are  
220 obvious in the highlighted part. However, C elements, resulting from the GO incorporation, were  
221 detected in the highlighted part in Fig. 7b, which shows a more densified matrix with less pores

222 or voids compared with that in Fig. 7a. Therefore, GO is definitely capable of filling the pores or  
 223 voids in the cement matrix and thus improves the mechanical behavior.

224

225 More importantly, the GO/CNTs/cement paste composite shows the highest compressive strength  
 226 (31.01 MPa), flexural strength (16.93 MPa) and Young's modulus (15.42 GPa), which is  
 227 improved by 21.13 %, 24.21% and 27.23 %, compared with cement paste, as shown in Fig. 6 and  
 228 Table 2. The reinforcement by the GO/CNTs composite is much higher than that by GO or CNTs  
 229 individually. Therefore, the GO/CNTs composite plays a more important role in reinforcing the  
 230 mechanical strength of cement paste, which is attributed to the better dispersion of CNTs in the  
 231 GO solution, as discussed and shown in Fig. 3 and Fig. 5. Better dispersion of CNTs, in turn,  
 232 contributes more to the mechanical enhancement of the cement paste.

233 **Table 2** Mechanical behavior of cement paste with different contents of CNTs and GO.

Specimen	Compressive strength (MPa)	Flexural strength (MPa)	Young's Modulus (GPa)
cement paste	25.60	13.64	12.12
0.05 wt. % CNTs/cement	27.24	15.06	12.63
0.05 wt. % GO/cement	28.43	15.85	14.31
0.025 wt. % GO/0.025 wt. % CNTs/cement	31.01	16.93	15.42

234

235 In order to verify the improved dispersion of CNTs with the help of GO in the cement paste  
 236 matrix, the microstructures of the CNTs/cement paste composite and the GO/CNTs/cement paste  
 237 composite were compared and investigated, as shown in Fig. 8. Some agglomeration of the  
 238 CNTs in the cement paste can be seen in Fig. 8a, otherwise the mechanical improvement should  
 239 be higher than the present results. However, the agglomeration of CNTs significantly disappears

240 in the GO/CNTs/cement paste composite, as shown in Fig. 8b. Most of the CNTs tend to be  
241 uniformly distributed in the pores or voids of the matrix, rather than intertwining with each other.  
242 Therefore, it is reasonable to deduce that the better dispersion of CNTs, resulting from the GO  
243 incorporation, is the basis for the stronger reinforcement of CNTs on the cement paste. More  
244 importantly, as seen in Fig. 8b and 8c, some GO sheets exist in the middle of the CNTs, which is  
245 like a bridge linking the dispersed CNTs together by chemical bonding. It is considered that the  
246 space interlocking of CNTs by GO incorporation also contributes to the mechanical improvement  
247 of cement paste.

248

249 FTIR analysis was conducted to investigate the chemical interaction between CNTs and GO  
250 sheets, as shown in Fig. 9. The characteristic peaks of GO at 1723, 1621, 1403, 1222 and 1058  
251  $\text{cm}^{-1}$  indicate carboxyl or carbonyl C=O stretching, H-O-H bending band of the absorbed  $\text{H}_2\text{O}$   
252 molecules, carboxyl O-H stretching, phenolic C-OH stretching and alkoxy C-O stretching [19].  
253 In addition, the characteristic peaks of CNTs at 2361, 1716, 1565, and 1182  $\text{cm}^{-1}$  indicate the O-  
254 H stretch from strongly hydrogen-bonded  $-\text{COOH}$ , C=O (carboxylic acid moieties), carboxylate  
255 anion stretching and C-O stretching, which shows the CNTs are decorated with carboxyl groups.  
256 However, the higher intensity and large width of these bands have the stronger interactions in the  
257 GO/CNTs composite. Particularly, the higher absorption at 1720  $\text{cm}^{-1}$ , corresponding to the  
258 stretching vibration of the C=O ester groups formed between the carboxylic acid groups of the  
259 CNTs and the alcohol groups of GO, indicates that the CNTs have indeed been covalently  
260 attached to the GO.

261

262 A number of research works have demonstrated the significant reinforcement mechanism of the  
263 cement matrix by CNTs or GO. Li et al. [7] indicated that chemical reactions took place between  
264 the carboxylic acid of CNTs and the calcium silicate hydrate (C-S-H) or  $\text{Ca}(\text{OH})_2$  of the cement  
265 matrix. The strong covalent force on the interface between the CNTs and matrix can improve the  
266 load-transfer efficiency from the cement matrix to the CNTs. Duan et al. [8] pointed out that GO  
267 sheets containing carboxylic acid groups can also form strong interfacial adhesion between the  
268 GO and the cement matrix, which has a similar reinforcement mechanism to CNTs. As a result,  
269 due to the excellent mechanical behavior of the functionalized CNTs and GO with better  
270 interaction with the cement matrix, the mechanical properties of the cement composite reinforced  
271 by GO or CNTs are clearly improved. In this study, it is the first time that the space interlocking  
272 mechanism of the GO/CNTs/cement paste composite with enhanced mechanical properties has  
273 been proposed, as shown in Fig. 10. The significant mechanical improvement of the  
274 GO/CNTs/cement paste composite is mainly attributed by two effects. Firstly, the better  
275 dispersion of CNTs ensures more CNTs contribute to the mechanical enhancement of cement  
276 paste.. Secondly, the two separate phases, (C-S-H) and  $\text{Ca}(\text{OH})_2$  in the cement hydration  
277 product, are likely linked by the GO and CNTs together. GO sheets can not only interlock the  
278 cement matrix together, but also bridge the CNTs by chemical bonding. More load can thus be  
279 transferred and shared by the GO and CNTs simultaneously. Finally, the improved chemical  
280 bonding among the CNTs by GO incorporation can result in a space interlocking structure, the  
281 [CNTs-GO-CNTs] structure, which helps to improve the load-transfer efficiency from the cement  
282 matrix to the GO/CNTs composites. As a result, the mechanical properties of the  
283 GO/CNTs/cement paste composite are significantly improved.

284

#### 285 4. Conclusions

286 This paper presents the co-effects of GO/CNTs composites on the mechanical properties of  
287 cement paste. The UV-vis spectroscopy and optical microscopy results show that the dispersion  
288 of CNTs in GO solution is much better than in aqueous solution due to the higher electrostatic  
289 repulsion. In addition, the flexural and compressive strength of cement paste are greatly  
290 increased by 21.13 % and 24.21% with the incorporation of 0.025 wt. % CNTs/ 0.025 wt. % GO  
291 composites, which is much higher than that reinforced by 0.05 wt. % CNTs (6.40 % and 10.14  
292 %) or 0.05 wt. % GO (11.05% and 16.20 %), respectively. More CNTs contribute to the  
293 mechanical enhancement of cement paste due to the better dispersion by GO incorporation, and  
294 the improved interaction among the CNTs by GO addition can help to transfer more load from  
295 cement matrix to the CNTs or GO, which results in the mechanical behavior of cement paste  
296 improving significantly. Finally, the space interlocking mechanism of the GO/CNTs/cement  
297 paste composite with enhanced mechanical property is proposed.

#### 298 Acknowledgements

299 The authors would like to acknowledge the financial support from the Hong Kong Research  
300 Grant Council under the Grant 615810, the China Ministry of Science and Technology under the  
301 Grant 2015CB655100, Information Technology of Guangzhou under the Grant 2013J4500069  
302 and the Natural Science Foundation of China under the Grant 51302104.

#### 303 References

- 304 [1] Z. Lu, J. Zhang, G. Sun, B. Xu, Z. Li, C. Gong, Effects of the form-stable expanded  
305 perlite/paraffin composite on cement manufactured by extrusion technique, *Energy*, (2015).  
306 [2] M.S. Konsta-Gdoutos, Z.S. Metaxa, S.P. Shah, Highly dispersed carbon nanotube reinforced  
307 cement based materials, *Cement and Concrete Research*, 40 (2010) 1052-1059.  
308 [3] M.S. Konsta-Gdoutos, Z.S. Metaxa, S.P. Shah, Multi-scale mechanical and fracture  
309 characteristics and early-age strain capacity of high performance carbon nanotube/cement  
310 nanocomposites, *Cement and Concrete Composites*, 32 (2010) 110-115.

- 311 [4] S. Parveen, S. Rana, R. Fangueiro, M.C. Paiva, Microstructure and mechanical properties of  
312 carbon nanotube reinforced cementitious composites developed using a novel dispersion  
313 technique, *Cement and Concrete Research*, 73 (2015) 215-227.
- 314 [5] B. Zou, S.J. Chen, A.H. Korayem, F. Collins, C. Wang, W.H. Duan, Effect of ultrasonication  
315 energy on engineering properties of carbon nanotube reinforced cement pastes, *Carbon*, 85  
316 (2015) 212-220.
- 317 [6] A. Cwirzen, K. Habermehl-Cwirzen, V. Penttala, Surface decoration of carbon nanotubes and  
318 mechanical properties of cement/carbon nanotube composites, *Advances in cement research*, 20  
319 (2008) 65-73.
- 320 [7] G.Y. Li, P.M. Wang, X. Zhao, Mechanical behavior and microstructure of cement composites  
321 incorporating surface-treated multi-walled carbon nanotubes, *Carbon*, 43 (2005) 1239-1245.
- 322 [8] Z. Pan, L. He, L. Qiu, A.H. Korayem, G. Li, J.W. Zhu, F. Collins, D. Li, W.H. Duan, M.C.  
323 Wang, Mechanical properties and microstructure of a graphene oxide–cement composite,  
324 *Cement and Concrete Composites*, 58 (2015) 140-147.
- 325 [9] M. Saafi, L. Tang, J. Fung, M. Rahman, J. Liggat, Enhanced properties of graphene/fly ash  
326 geopolymeric composite cement, *Cement and Concrete Research*, 67 (2015) 292-299.
- 327 [10] J. Du, H.M. Cheng, The fabrication, properties, and uses of graphene/polymer composites,  
328 *Macromolecular Chemistry and Physics*, 213 (2012) 1060-1077.
- 329 [11] D. Li, M.B. Müller, S. Gilje, R.B. Kaner, G.G. Wallace, Processable aqueous dispersions of  
330 graphene nanosheets, *Nature nanotechnology*, 3 (2008) 101-105.
- 331 [12] S. Musso, J.-M. Tulliani, G. Ferro, A. Tagliaferro, Influence of carbon nanotubes structure  
332 on the mechanical behavior of cement composites, *Composites Science and Technology*, 69  
333 (2009) 1985-1990.
- 334 [13] J. Yu, N. Grossiord, C.E. Koning, J. Loos, Controlling the dispersion of multi-wall carbon  
335 nanotubes in aqueous surfactant solution, *Carbon*, 45 (2007) 618-623.
- 336 [14] L. Qiu, X. Yang, X. Gou, W. Yang, Z.F. Ma, G.G. Wallace, D. Li, Dispersing carbon  
337 nanotubes with graphene oxide in water and synergistic effects between graphene derivatives,  
338 *Chemistry-A European Journal*, 16 (2010) 10653-10658.
- 339 [15] X. Fan, W. Peng, Y. Li, X. Li, S. Wang, G. Zhang, F. Zhang, Deoxygenation of exfoliated  
340 graphite oxide under alkaline conditions: a green route to graphene preparation, *Advanced  
341 Materials*, 20 (2008) 4490-4493.
- 342 [16] S. Chuah, Z. Pan, J.G. Sanjayan, C.M. Wang, W.H. Duan, Nano reinforced cement and  
343 concrete composites and new perspective from graphene oxide, *Construction and Building  
344 Materials*, 73 (2014) 113-124.
- 345 [17] S. Lv, Y. Ma, C. Qiu, T. Sun, J. Liu, Q. Zhou, Effect of graphene oxide nanosheets of  
346 microstructure and mechanical properties of cement composites, *Construction and building  
347 materials*, 49 (2013) 121-127.
- 348 [18] E. Horszczaruk, E. Mijowska, R.J. Kalenczuk, M. Aleksandrak, S. Mijowska,  
349 Nanocomposite of cement/graphene oxide–Impact on hydration kinetics and Young’s modulus,  
350 *Construction and Building Materials*, 78 (2015) 234-242.
- 351 [19] M. Cano, U. Khan, T. Sainsbury, A. O’Neill, Z. Wang, I.T. McGovern, W.K. Maser, A.M.  
352 Benito, J.N. Coleman, Improving the mechanical properties of graphene oxide based materials  
353 by covalent attachment of polymer chains, *Carbon*, 52 (2013) 363-371.

354

355

### Figure Captions

**Fig. 1.** XRD patterns of graphite and GO.

**Fig. 2.** XPS C 1s spectra of GO.

**Fig. 3.** UV–vis spectroscopy results of (a) CNTs/aqueous and (b) CNTs/GO solutions.

**Fig. 4.** Scheme showing the dispersion of (a) unfunctionalized CNTs; (b) functionalized CNTs in the aqueous solution and (c) functionalized CNTs in the GO solution.

**Fig. 5.** Typical optical microscope images for (a) CNTs/aqueous and (b) CNTs/GO solutions.

**Fig. 6.** (a) Compressive and (b) flexural strength of the specimens.

**Fig. 7.** SEM images and EDX results of GO/cement paste (a) highlighted part without GO; (b) highlighted part with GO.

**Fig. 8.** SEM images of (a) CNTs/cement paste composite and (b) GO/CNTs/cement paste composite with low magnification and (c) high magnification.

**Fig. 9.** FTIR spectra of the GO, CNTs and the GO/CNTs composite.

**Fig. 10.** Mechanism of GO/CNTs/cement paste composite with enhanced mechanical properties.

### Figures

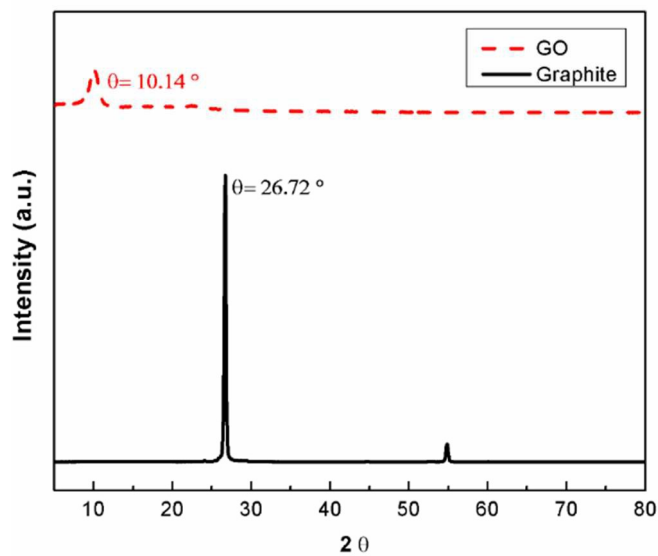


**Fig. 1.** XRD patterns of graphite and GO.

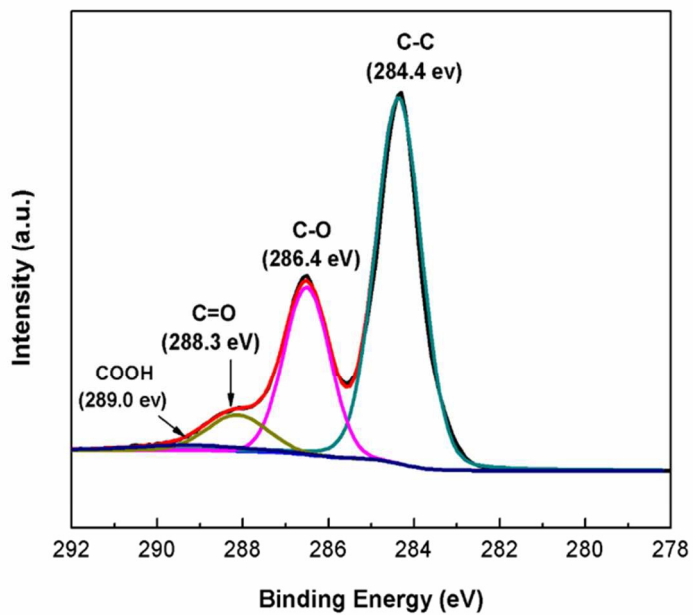


**Fig. 2.** XPS C 1s spectra of GO.

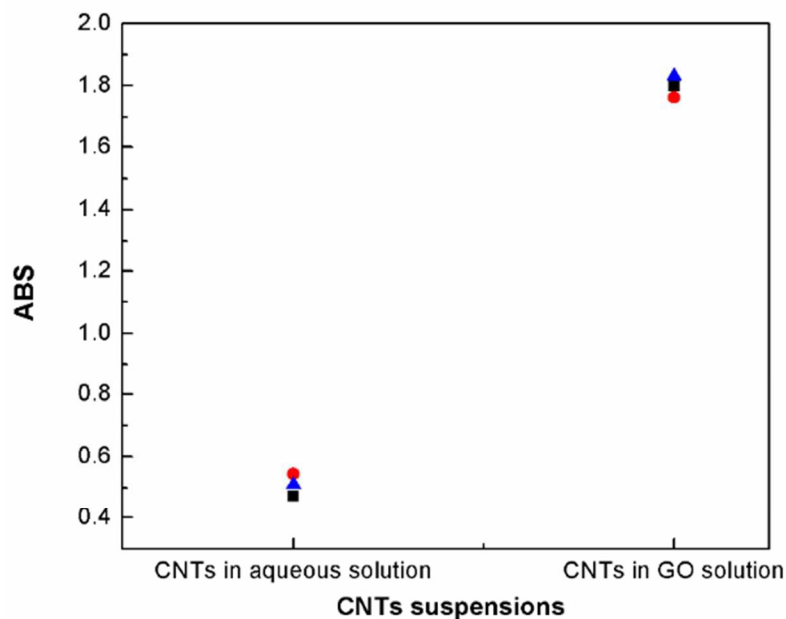


**Fig. 3.** UV-vis spectroscopy results of (a) CNTs/aqueous and (b) CNTs/GO solutions.

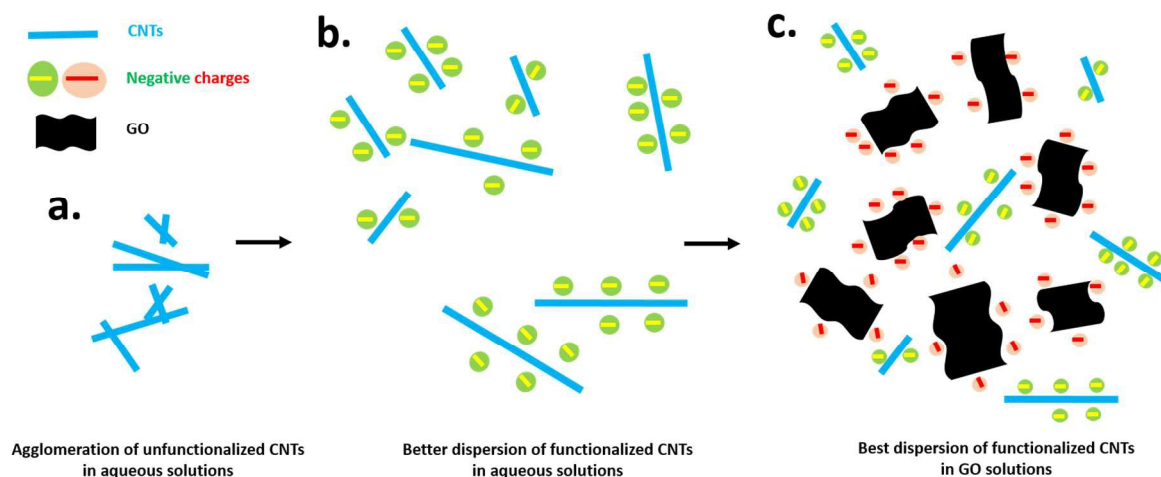


**Fig. 4.** Scheme showing the dispersion of (a) unfunctionalized CNTs; (b) functionalized CNTs in the aqueous solution and (c) functionalized CNTs in the GO solution.

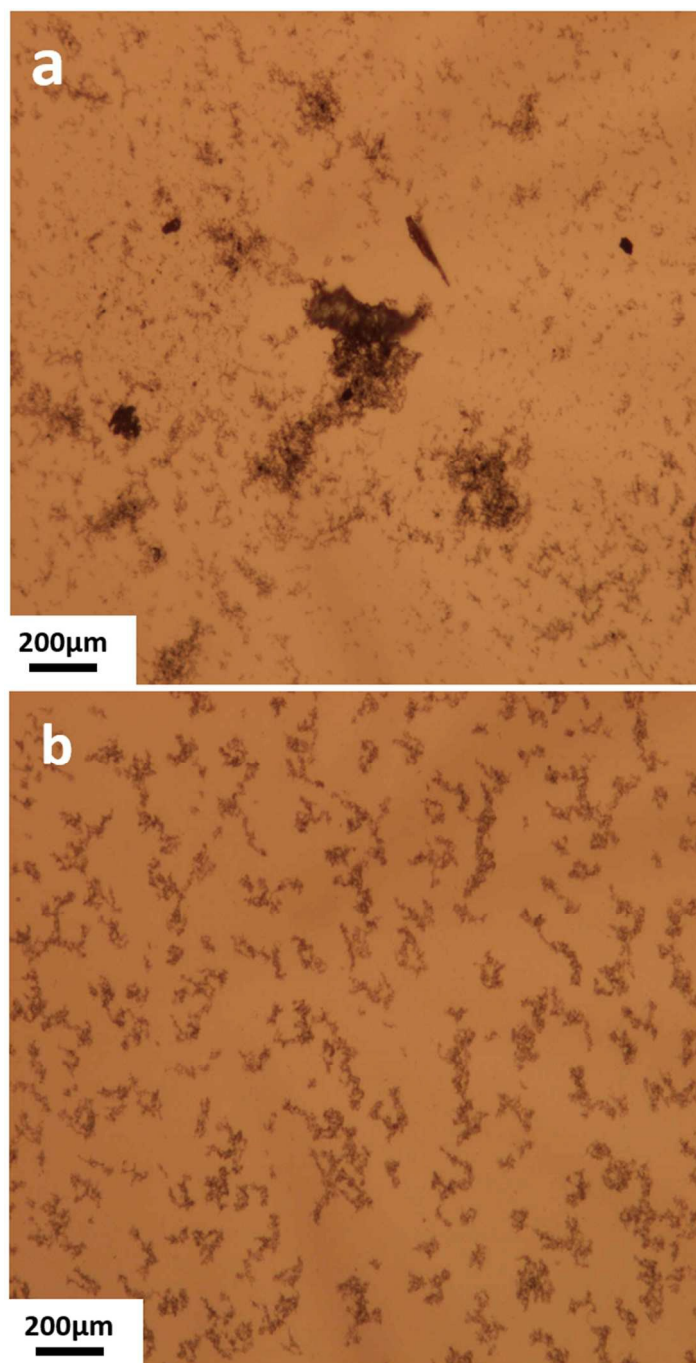


**Fig. 5.** Typical optical microscope images for (a) CNTs/aqueous and (b) CNTs/GO solutions.

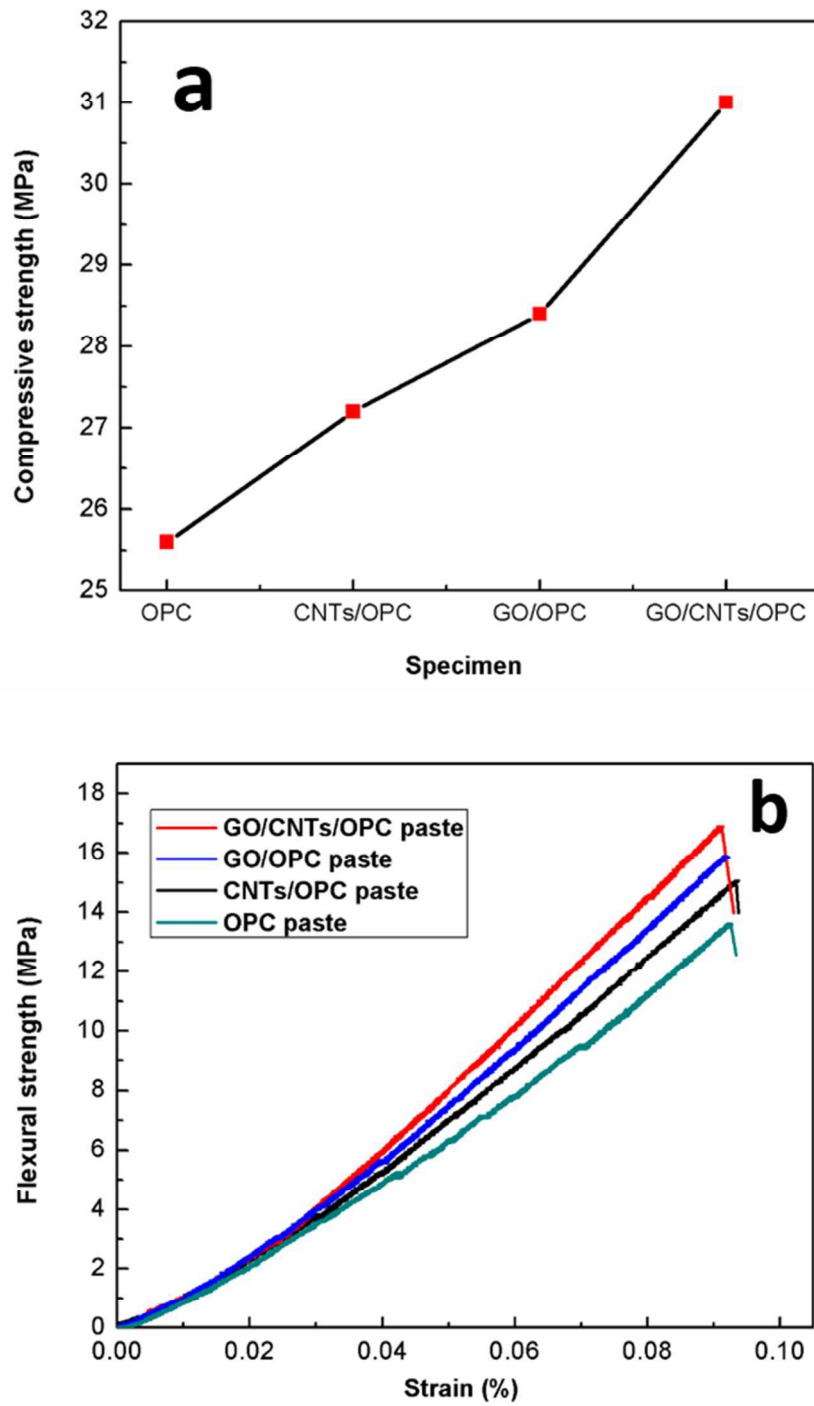
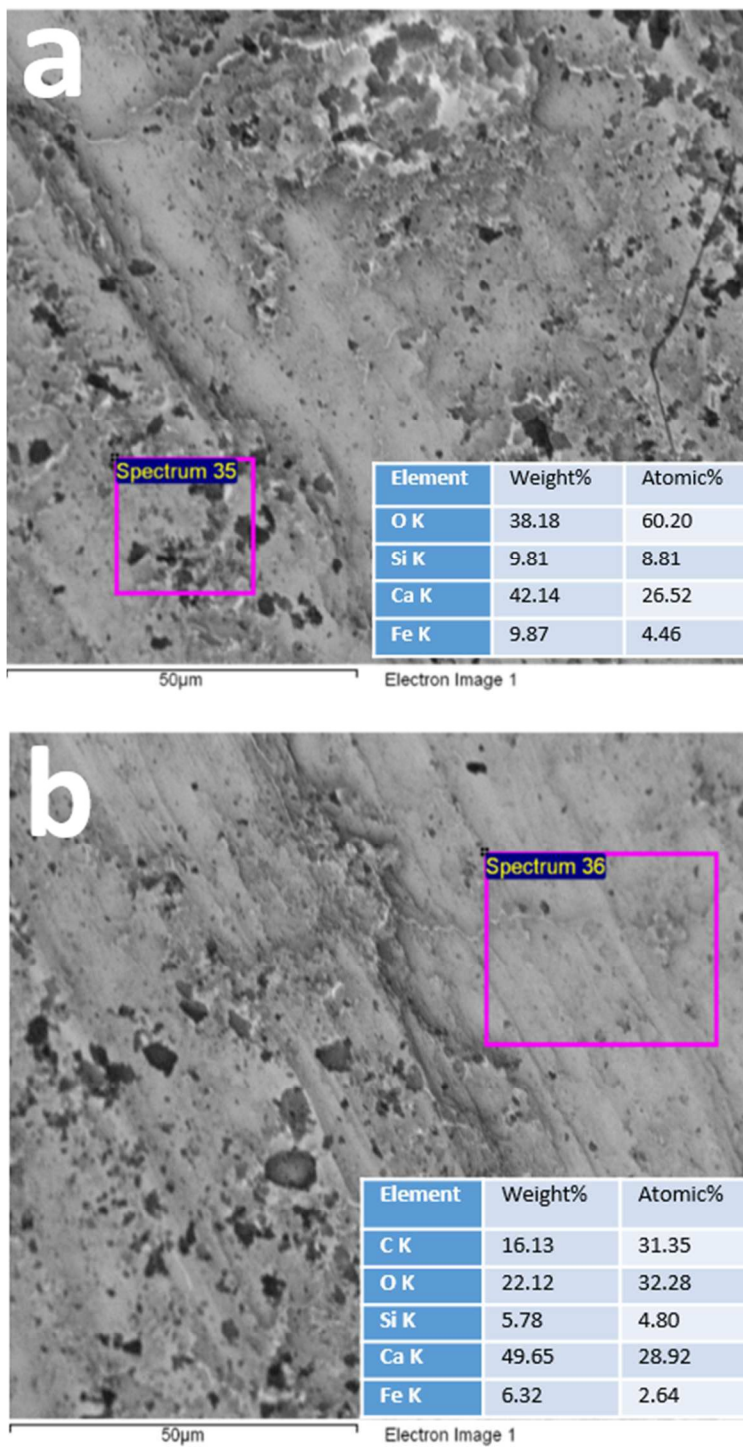
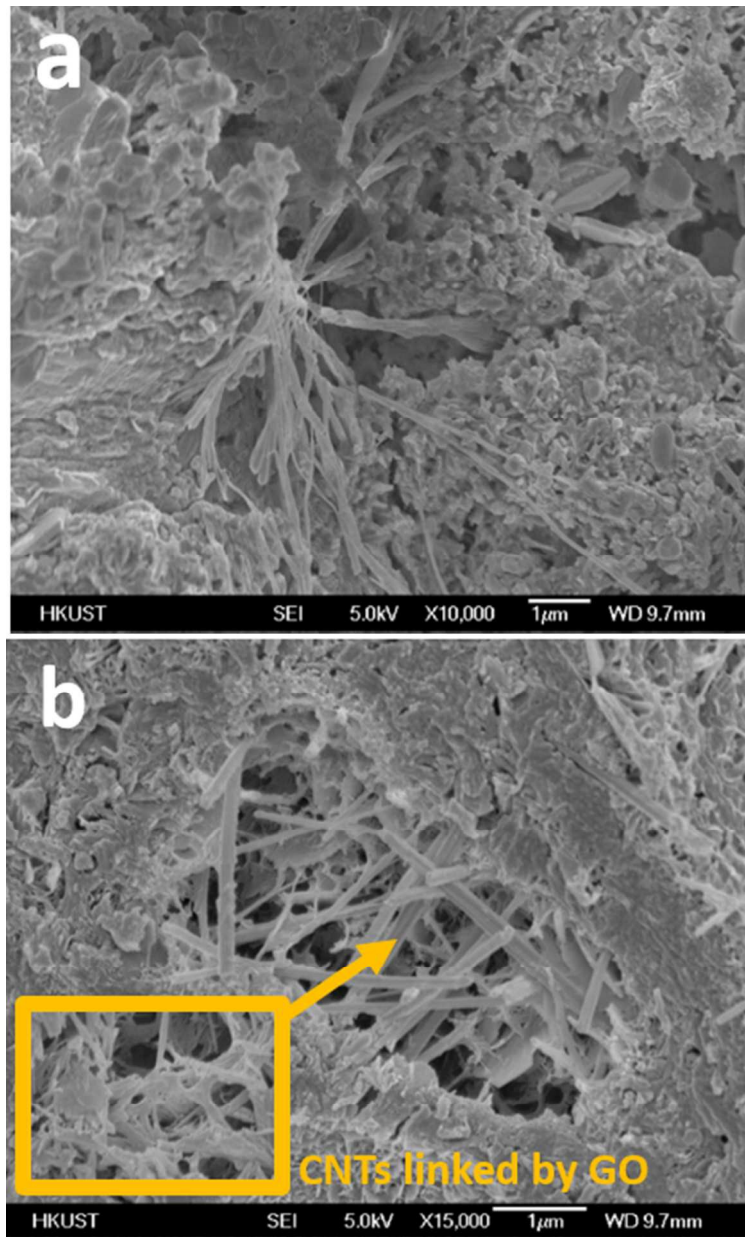
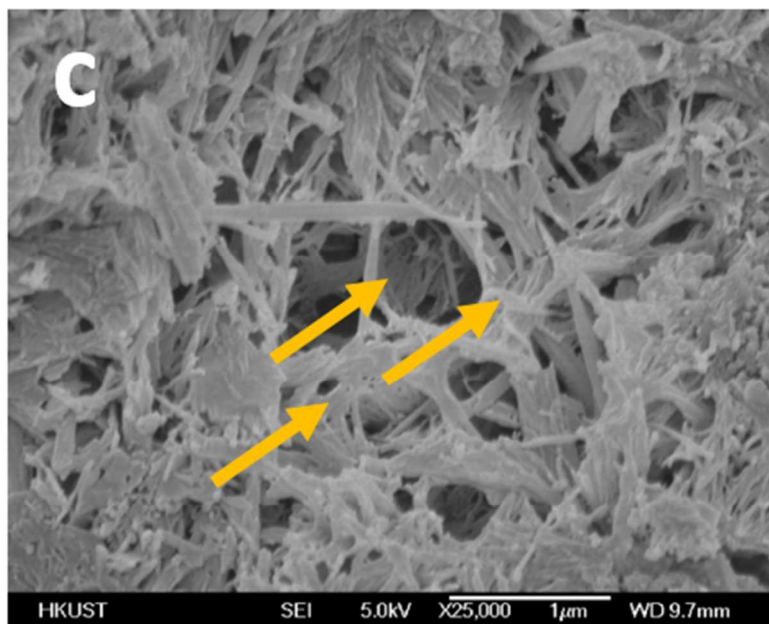


Fig. 6. (a) Compressive and (b) flexural strength of the specimens.



**Fig. 7.** SEM/EDX results of GO/cement paste (a) highlighted part without GO; (b) highlighted part with GO.





**Fig. 8.** SEM images of (a) CNTs/cement paste composite and (b) GO/CNTs/cement paste composite with low magnification and (c) high magnification.

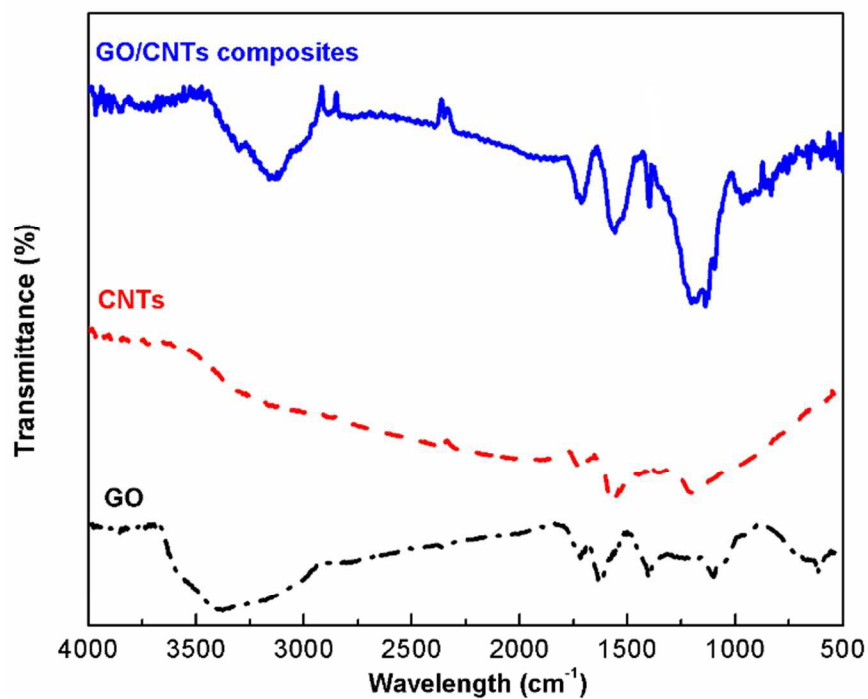


**Fig. 9.** FTIR spectra of the GO, CNTs and the GO/CNTs composite.

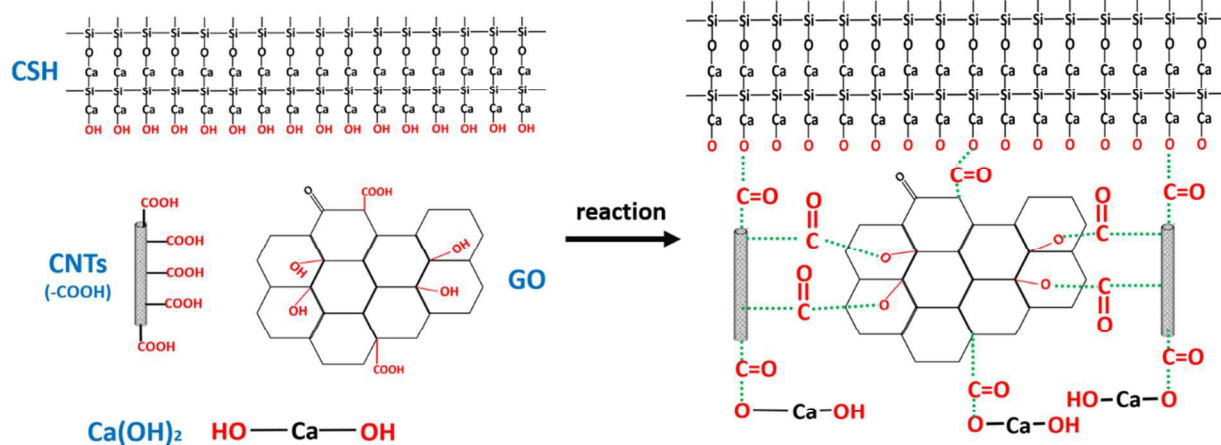


Fig. 10. Mechanism of GO/CNTs/cement paste composite with enhanced mechanical properties.